

JOINT METAL ARTIFACT REDUCTION AND SEGMENTATION OF CT IMAGES USING DICTIONARY-BASED IMAGE PRIOR AND CONTINUOUS-RELAXED POTTS MODEL

Pengchong Jin, Dong Hye Ye, Charles A. Bouman

School of Electrical and Computer Engineering, Purdue University, West Lafayette, IN, USA, 47907

ABSTRACT

Segmenting interesting objects from CT images has a wide range of applications. However, to achieve good results, it is often necessary to apply metal artifact reduction to raw CT images before segmentation. While there has been a great deal of research focusing on metal artifact reduction and segmentation as individual tasks, there have been very few attempts to solve the two problems jointly. We present a novel approach to solve the problem of segmenting raw CT images with metal artifacts, without the access to the raw CT data. Given an approximate metal artifact mask, the problem is formulated as a joint optimization over the restored image and the segmentation label, and the cost function includes a dictionary-based image prior to regularize the restored image and a continuous-relaxed Potts model for multi-class segmentation. An effective alternating method is used to solve the resulting optimization problem. The algorithm is applied to both simulated and real datasets and results show that it is effective in reducing metal artifacts and generating better segmentations simultaneously.

Index Terms— Metal Artifact Reduction, Potts Model Segmentation, Dictionary Learning, Security CT

1. INTRODUCTION

Computed Tomography (CT) has a wide range of applications in medical diagnosis [1] and security inspection [2]. In many of these applications, it is important and necessary to segment CT images for further analysis. For example, segmentation of anatomical structure is a critical step in image guided radiotherapy or the design of custom bone replacements. Segmentation is also of great importance in security applications where objects are segmented before target classification.

However, raw CT images often contain artifacts such as streaks due to dense metal objects, and these artifacts can make accurate segmentation difficult. In the past decades, people have developed various metal artifact reduction (MAR)

techniques to correct the image. Perhaps the most well-known approaches in MAR are based on sinogram correction (SC-MAR). These methods typically correct the metal trace in the raw CT data by using either sinogram inpainting [3, 4] or the knowledge obtained from the projection of a prior image that is derived from the original CT image [5–7]. The final image of SC-MAR is then produced by reconstructing the restored sinogram. Alternatively, if the original CT data is not available, MAR can be done in the image domain (ID-MAR). Some ID-MAR methods produce the corrected image by utilizing a pseudo sinogram from the projection of the original CT image [4]. Others identify the metal artifact regions in the image and apply image restoration techniques to do the correction [8].

On the other side, there have also been a variety of methods proposed for segmentation by using graph cut [9], shape prior [10], active contour [11], Mumford-Shah functional [12] etc.. Perhaps, the most related work in CT applications is [13], which is based on the method of isoperimetric graph partitioning [14]. The algorithm searches for splits within the connected components recursively until it is unable to find a strong separation. However, it does not fully explore the metal artifact structure in the CT image. Surprisingly, while a great deal of research has been done in metal artifact reduction and segmentation as individual tasks, relatively little research has considered the two problems jointly.

In this paper, we propose a novel approach to the segmentation of CT images with metal artifacts, and with no access to the raw CT data. Our method is based on the joint estimation of both the restored image and the segmentation in a unified optimization framework. The unified cost function consists of three terms: 1) a data fidelity term that relates the raw and restored image and incorporates a streak mask; 2) a dictionary-based image prior which regularizes the restored image; 3) a term based on the continuous-relaxed Potts model which couples the restored image intensities and segmentation labels. We derive an alternating optimization algorithm to minimize the overall cost function and the result of this procedure produces a joint restoration and segmentation of the image. We present results using both simulated and real CT dataset and demonstrate that the joint MAR and segmentation can produce better results than the sequential ID-MAR and segmentation method, without the use of the raw CT data.

This material is based upon work supported by the U.S. Department of Homeland Security, Science and Technology Directorate, Office of University Programs, under Grant Award 2013-ST-061-ED0001. The views and conclusions contained in this document are those of the authors and should not be interpreted as necessarily representing the official policies, either expressed or implied, of the U.S. Department of Homeland Security.

2. JOINT METAL ARTIFACT REDUCTION AND SEGMENTATION

Let $x^{(\text{orig})} \in \mathbb{R}^N$ be the input CT image with metal artifacts. Assume K target material intensities $\mu \in \mathbb{R}^K$ is given and a binary artifact mask $b \in \{0, 1\}^N$, defined as

$$b_i = \begin{cases} 1 & \text{if the } i\text{-th pixel has artifact} \\ 0 & \text{otherwise} \end{cases}, \quad (1)$$

is obtained in advance. Our objective is to use $x^{(\text{orig})}$, μ and b to produce an output image x which has reduced metal artifacts and a segmentation label vector $z \in \{1, \dots, K\}^N$ of K materials over the image.

We formulate this problem as the joint optimization problem of the restored image and the segmentation. Mathematically, the overall cost function can be written as

$$\min_{x, z} \left\{ \frac{1}{2} \sum_{i=1}^N (1 - b_i) (x_i - x_i^{(\text{orig})})^2 + J_I(x) + \frac{\beta}{2} \sum_{i=1}^N \sum_{k=1}^K w_i \delta(z_i - k) (x_i - \mu_k)^2 + \lambda \sum_{\{i, j\} \in \mathbb{C}} (1 - \delta(z_i - z_j)) \right\} \quad (2)$$

where $\delta(\cdot)$ is the delta function, \mathbb{C} represents the set of all neighboring pixel pairs, and β , λ are the regularization weights. Here $J_I(x)$ denotes the image domain prior which is used to balance the local smoothness and edge structures. We also add the weights w_i , defined as

$$w_i = \begin{cases} w & \text{if } b_i = 1 \\ 1 & \text{if } b_i = 0 \end{cases}, \quad (3)$$

to control the segmentation term in artifact and non-artifact regions.

Notice that the optimization over the segmentation label z only involves the last two terms, which is essentially the MAP segmentation based on the discrete Potts model. However, due to the non-convexity, this solution can often be trapped into a local minimum which can lead to poor segmentation result. Instead, we use an approach similar to [15] and propose a continuous-relaxed version of the discrete Potts model. In particular, we relax the $\delta(z_i - k)$ to be a probability measure u_i for each i , and the overall problem becomes the following constrained optimization:

$$\min_{x, u} \left\{ \frac{1}{2} \sum_{i=1}^N (1 - b_i) (x_i - x_i^{(\text{orig})})^2 + J_I(x) + \frac{\beta}{2} \sum_{i=1}^N \sum_{k=1}^K w_i u_{i,k} (x_i - \mu_k)^2 + \lambda \sum_{\{i, j\} \in \mathbb{C}} \sum_{k=1}^K |u_{i,k} - u_{j,k}| \right\}$$

$$\text{subject to } 0 \leq u_{i,k} \leq 1, \sum_{k=1}^K u_{i,k} = 1. \quad (4)$$

Once we have the optimal u , the segmentation label can be obtained by picking up the label with the largest probability,

$$z_i \leftarrow \arg \max_{k \in \{1, \dots, K\}} u_{i,k}. \quad (5)$$

Lastly, the image domain prior $J_I(x)$ regularizes the local image behavior and serves to fill in correct pixel values in the metal artifact region. Several image priors have been proposed in different image processing applications [16–18]. We construct the term $J_I(x)$ by representing all the overlapped patches as the sparse combination of entries from a globally learned dictionary Φ using K-SVD algorithm [17]. Loosely speaking, it assumes that

$$R_i x \approx \Phi \nu_i, \text{ with } \|\nu_i\|_0 \leq T \quad (6)$$

where Φ is the global over-complete dictionary, R_i is the matrix to extract a patch located at the i -th pixel, ν_i is the corresponding sparse coefficient vector, and T is the specified sparsity constraint. Under certain conditions [19], it is equivalent to solve an unconstrained optimization with the l_0 norm replaced by l_1 . Substituting the image prior into $J_I(x)$ in (4), we obtain the final optimization problem as follows

$$\min_{x, u, \nu} \left\{ \frac{1}{2} \sum_{i=1}^N (1 - b_i) (x_i - x_i^{(\text{orig})})^2 + \frac{\alpha}{2} \sum_{i=1}^N \|R_i x - \Phi \nu_i\|_2^2 + \sum_{i=1}^n \gamma_i \|\nu_i\|_1 + \frac{\beta}{2} \sum_{i=1}^N \sum_{k=1}^K w_i u_{i,k} (x_i - \mu_k)^2 + \lambda \sum_{\{i, j\} \in \mathbb{C}} \sum_{k=1}^K |u_{i,k} - u_{j,k}| \right\} \quad (7)$$

subject to $0 \leq u_{i,k} \leq 1, \sum_{k=1}^K u_{i,k} = 1$

where α and γ_i are additional regularization weights.

We use alternating optimizing to solve (7). The inputs of the algorithm are the original image $x^{(\text{orig})}$, the artifact mask b , the globally learned dictionary Φ for image patches, the mean intensities μ of K materials, and the regularization weights α , β , γ_i and w_i . At the initialization step, we set the image $x \leftarrow x^{(\text{orig})}$, and $u_{i,k} \leftarrow \frac{1}{K}$ for all i and k . Firstly, fixing x and u , optimization over ν can be solved patch-wise using the standard sparse coding techniques, such as Orthogonal Matching Pursuit (OMP) [20]. Then, with ν and u fixed, we optimize over the image x . If we denote $U \in \mathbb{R}^{N \times K}$ as the matrix whose entries are $u_{i,k}$, W and D as the diagonal matrices whose diagonal entries are w_i and $1 - b_i$ respectively, then the image update can be written in the compact form as

$$\min_x \left\{ \frac{1}{2} \|x - x^{(\text{orig})}\|_D^2 + \frac{\alpha}{2} \sum_{i=1}^N \|R_i x - \Phi \nu_i\|_2^2 + \frac{\beta}{2} \|x - U \mu\|_W^2 \right\}, \quad (8)$$

and its solution is given by

$$x \leftarrow \left(D + \beta W + \alpha \sum_{i=1}^N R_i^T R_i \right)^{-1} \left(Dx^{(\text{orig})} + \beta W U \mu + \alpha \sum_{i=1}^N R_i^T \Phi \nu_i \right) \quad (9)$$

Despite its complicated form, (9) is nothing but the weighted average of all the overlapped patches with some additional pixel-wise regularization, and the update in (9) can be implemented very efficiently using pixel-wise division. Finally, fixing ν and x , we solve the constrained optimization over u given by

$$\min_u \left\{ \frac{\beta}{2} \|x - U\mu\|_W^2 + \lambda \sum_{\{i,j\} \in \mathcal{C}} \sum_{k=1}^K |u_{i,k} - u_{j,k}| \right\}$$

subject to $0 \leq u_{i,k} \leq 1, \sum_{k=1}^K u_{i,k} = 1.$ (10)

The optimization (10) can be solved using the effective continuous max-flow algorithm in [15], which converts the problem into the convex optimization problem.

3. IDENTIFY METAL ARTIFACTS IN CT IMAGES

We propose the forward and backward projection method to generate the binary artifact mask b as follows.

- Step 1: Generate the high density image $x^{(\text{high})}$

$$x_i^{(\text{high})} \leftarrow x_i^{(\text{orig})} \delta(x_i^{(\text{orig})} \geq L^{(\text{high})}) \quad (11)$$

where $L^{(\text{high})}$ is the threshold for high density pixels.

- Step 2: Apply the forward Radon transform to $x^{(\text{orig})}$ and $x^{(\text{high})}$ separately to obtain two projections:

$$p^{(\text{high})} \leftarrow Ax^{(\text{high})}, p^{(\text{orig})} \leftarrow Ax^{(\text{orig})} \quad (12)$$

where A represents the forward projection matrix.

- Step 3: Correct the high density projection with the parameter $r \geq 1$.

$$p_i^{(\text{corr})} = \frac{p_i^{(\text{high})}}{p_i^{(\text{orig})}} p_i^{(\text{high})^r} = \frac{p_i^{(\text{high})^{1+r}}}{p_i^{(\text{orig})}} \quad (13)$$

- Step 4: Apply Filter Back-projection (FBP) to the corrected projection and thresholding.

$$b' \leftarrow \text{FBP}(p^{(\text{corr})}) \quad (14)$$

$$b \leftarrow \delta(b'_i > L^{(\text{artifact})}) \delta(x_i^{(\text{orig})} < L^{(\text{high})}) \quad (15)$$

where $L^{(\text{artifact})}$ is the threshold for metal artifact pixels.

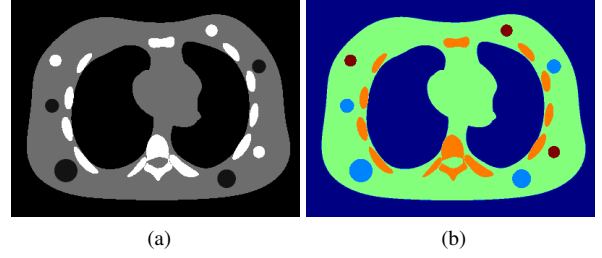


Fig. 1. the ground truth (a) intensity map, (b) segmentation, of the simulated data, the display window of the intensity is $[-200, 400]$ HU; the segmentation label is color-coded.

Method	RMSE (HU)	Sørensen-Dice score
baseline	136.9830	0.8828
sequential MAR/seg.	167.2736	0.9135
joint MAR/seg.	99.3498	0.9382

Table 1. Quantitative comparison of different methods. The RMSE is calculated over pixels between $[0, 4500]$ HU. The Sørensen-Dice scores [23] are averaged over all the labels.

4. RESULTS

We present three methods for comparison. The first is the baseline method where we apply segmentation [15] on the raw CT images. The second is the sequential MAR/segmentation where the image goes through an image restoration algorithm [21] followed by the segmentation [15]. The last is the proposed joint MAR/segmentation method. We terminate the iteration of the joint method when the average pixel update is less than 0.1 HU.

The first dataset is a simulated dataset based on [22]. The ground truth intensity and segmentation maps are shown in Figure 1. The raw CT image is shown in Figure 2b. We set $L^{(\text{high})} = 2500$ HU and $L^{(\text{artifact})} = 200$ HU and the artifact mask is shown in Figure 2a. We use K-SVD algorithm with $T = 3$ to learn the dictionary from 9×9 patches from the raw input image. The input mean intensities are $\mu = [0, 850, 1050, 3500, 4700]^T$ HU. Figure 2 shows the comparison of different methods. The raw CT image in Figure 2b contains many streak artifacts due to metal, and the resulting segmentation in Figure 2c is inaccurate in the artifact regions. In Figure 2d and 2e, while applying the restoration followed by segmentation can reduce some artifacts, it is sensitive to the mask and can not generate a good segmentation directly. In contrast, the output of the proposed algorithm in Figure 2f and 2g gives better results. Major metal artifacts are reduced and the segmentation is more accurate. The quantitative result in Table 1 also suggests the proposed method generates better image and segmentation.

The second dataset is a real baggage CT image. Figure 3b shows the raw image, which contains strong streak artifacts

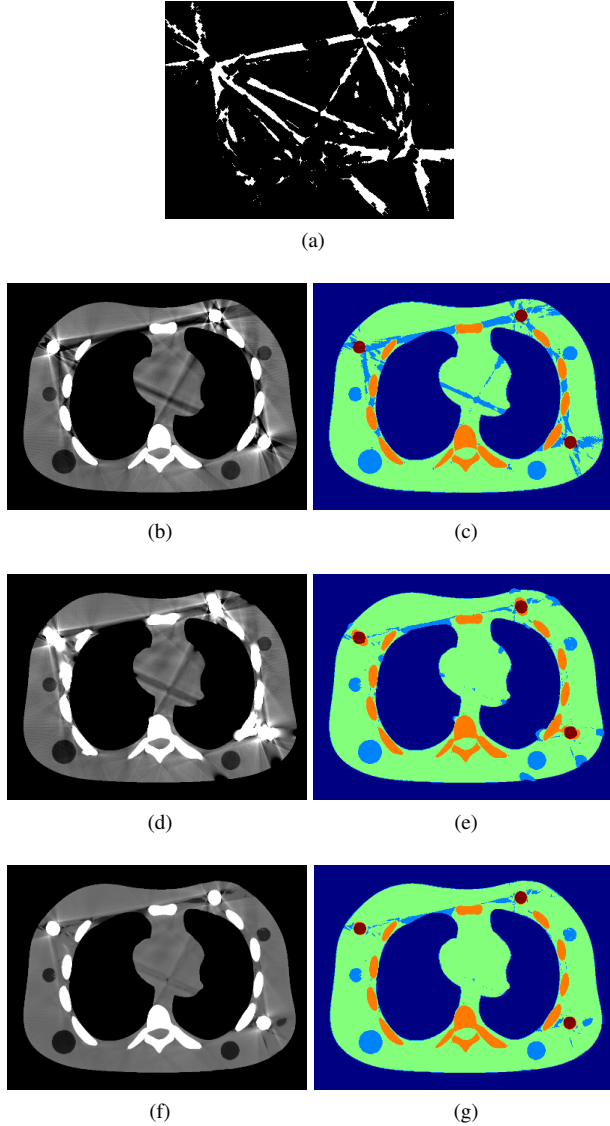


Fig. 2. (a) the artifact mask, (b), (c) the image and segmentation of baseline (d), (e) the image and segmentation of sequential MAR/seg. (f), (g) the image and segmentation of joint MAR/seg. the display window $[-200, 400]$ HU; the segmentation is color-coded.

due to the metal. We set $L^{(\text{high})} = 2500$ HU and $L^{(\text{artifact})} = 50$ HU and Figure 3a shows the artifact mask. We set the mean intensities to be $\mu = [0, 600, 1000, 1150, 1400, 3000]^T$ HU. Figure 3c shows the segmentation on the raw CT image and notice that objects are split due to the streak artifact. Figure 3d and 3e show the results of applying the restoration algorithm followed by segmentation separately. While the restoration algorithm fills in the correct values in some artifact regions, it introduces extra artifacts, such as the region around the thin sheet on top left. This leads to the inaccurate segmentation in Figure 3e. On the other side, the major metal streak artifacts are corrected in the output image of the pro-

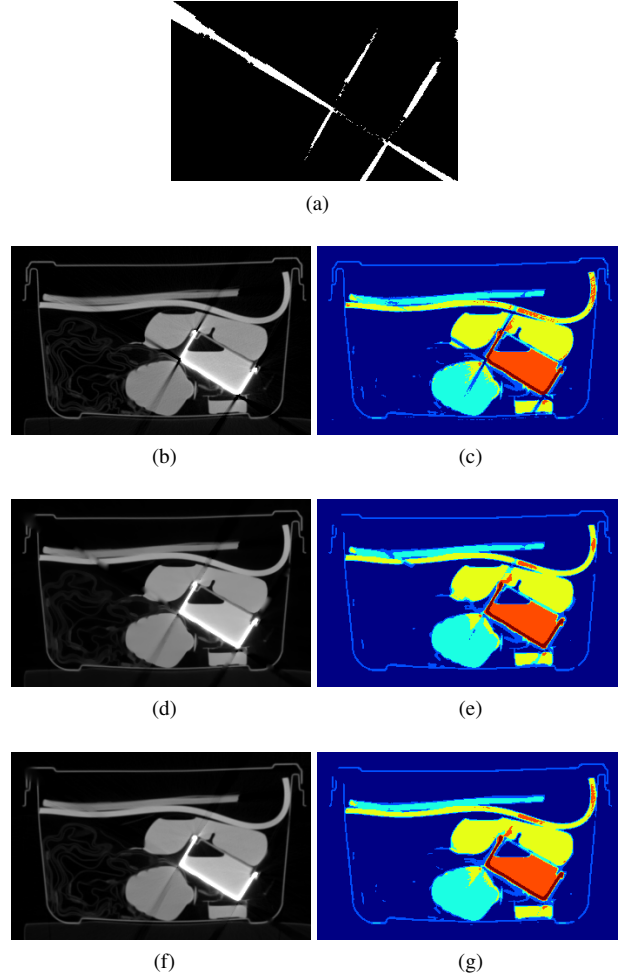


Fig. 3. (a) the artifact mask, (b), (c) the image and segmentation of baseline (d), (e) the image and segmentation of the sequential MAR/seg. (f), (g) the image and segmentation of the joint MAR/seg. the display window $[-1000, 1000]$ HU; the segmentation is color-coded.

posed algorithm in Figure 3f. Furthermore, the joint method merges the objects that were originally split and produces a more accurate segmentation in Figure 3g.

5. CONCLUSIONS

In this paper, we consider the problem of segmentation of CT images with metal artifacts and with no access to the CT data. We present a novel approach based on a joint estimation over image and segmentation in a unified optimization framework. By alternating optimization, the algorithm is able to improve both the image quality and segmentation simultaneously. Results on both simulated and real datasets show that the method is effective in reducing metal artifact and producing better segmentation than the sequential ID-MAR and segmentation, without the use of the raw CT data.

6. REFERENCES

- [1] J.-B. Thibault, K. D. Sauer, C. A. Bouman, and J. Hsieh, "A three-dimensional statistical approach to improved image quality for multislice helical CT," *Med. Phys.*, vol. 34, no. 11, pp. 4526–4544, Nov. 2007.
- [2] P. Jin, E. Haneda, C. A. Bouman, and K. D. Sauer, "A model-based 3D multi-slice helical CT reconstruction algorithm for transportation security application," in *Proc. 2nd Intl. Mtg. on image formation in X-ray CT*, 2012, pp. 297–300.
- [3] Y. Kim, S. Yoon, and J. Yi, "Effective sinogram inpainting for metal artifact reduction in X-ray CT images," in *IEEE Conf. Image Processing (ICIP)*, 2010, pp. 597–600.
- [4] H. K. Tuy, "A post-processing algorithm to reduce metallic clip artifacts in CT images," *Eur. Radiol.*, , no. 3, pp. 129–134, 1993.
- [5] E. Meyer, R. Raupach, M. Lell, B. Schmidt, and M. Kachelriess, "Normalized metal artifact reduction (NMAR) in computed tomography," *Med. Phys.*, , no. 10, pp. 5482–5493, Oct. 2010.
- [6] E. Meyer, R. Raupach, M. Lell, B. Schmidt, and M. Kachelriess, "Frequency split metal artifact reduction (FSMAR) in computed tomography," *Med. Phys.*, pp. 1904–1916, Apr. 2012.
- [7] P. Jin, C. A. Bouman, and K. D. Sauer, "A method for simultaneous image reconstruction and beam hardening correction," in *IEEE Nuclear Science Symp. and Medical Imaging Conf.*, Seoul, Korea, 2013.
- [8] A. Anderla, D. Culibrk, G. Delso, and M. Mirkovic, "MR image based approach for metal artifact reduction in x-ray CT," *The Scientific World Journal*, 2013.
- [9] Y. Boykov and V. Kolmogorov, "An experimental comparison of min-cut/max-flow algorithms for energy minimization in vision," *IEEE Trans. Pattern Analysis and Machine Intelligence*, vol. 26, no. 9, pp. 1124–1137, 2004.
- [10] N. Vu and B. S. Manjunath, "Shape prior segmentation of multiple objects with graph cuts," in *IEEE Conf. Computer Vision and Pattern Recognition (CVPR)*, 2008.
- [11] W. Yu, P. Franchetti, Y. Chang, and T. Chen, "Fast and robust active contours for image segmentation," in *IEEE Conf. Image Processing (ICIP)*, 2010, pp. 641–644.
- [12] J. An and Y. Chen, "Region based image segmentation using a modified Mumford-Shah algorithm," in *Scale Space and Variational Methods in Computer Vision*, 2007, pp. 733–742.
- [13] L. Grady, V. Singh, T. Kohlberger, C. Alvino, and C. Bahlmann, "Automatic segmentation of unknown objects, with application to baggage security," in *Eur. Conf. Computer Vision (ECCV)*, 2012, pp. 430–444.
- [14] L. Grady and E. L. Schwartz, "Isoperimetric graph partitioning for image segmentation," *IEEE Trans. Pattern Analysis and Machine Intelligence*, vol. 28, no. 3, pp. 469–475, 2006.
- [15] J. Yuan, E. Bae, X. Tai, and Y. Boykov, "A continuous max-flow approach to Potts model," in *Eur. Conf. Computer Vision (ECCV)*, 2010, pp. 379–392.
- [16] P. Jin, E. Haneda, and C. A. Bouman, "Implicit Gibbs prior models for tomographic reconstruction," in *the 46th Asilomar Conf. Signals, Systems and Computers*, Pacific Grove, CA, Nov. 2012, pp. 613–616.
- [17] M. Aharon, M. Elad, and A. Bruckstein, "K-SVD: An algorithm for designing overcomplete dictionaries for sparse representation," *IEEE Trans. Signal Proc.*, vol. 54, no. 11, pp. 4311–4322, 2006.
- [18] R. Zhang, C.A. Bouman, J.-B. Thibault, and K.D. Sauer, "Gaussian mixture Markov random field for image denoising and reconstruction," in *Global Conference on Signal and Information Processing (GlobalSIP)*, 2013 *IEEE*, Dec 2013, pp. 1089–1092.
- [19] J. A. Tropp, "Just relax: Convex programming methods for subset selection and sparse approximation," *IEEE Trans. Info. Thoery*, vol. 51, no. 3, pp. 1030–1051, 2005.
- [20] Y. C. Pati, R. Rezaifar, and P. S. Krishnaprasad, "Orthogonal matching pursuit: Recursive function approximation with applications to wavelet decomposition," in *the 27th Asilomar Conf. Signals, Systems and Computers*, Pacific Grove, CA, 1993.
- [21] D. Garcia, "Robust smoothing of gridded data in one and higher dimensions with missing values," *Computational Statistics and Data Analysis*, vol. 54, pp. 1167–1178, 2010.
- [22] W. P. Segars, M. Mahesh, T. J. Beck, E. C. Frey, and B. M. W. Tsui, "Realistic CT simulation using the 4D XCAT phantom," *Med. Phys.*, vol. 35, no. 8, pp. 3800–3808, Aug. 2008.
- [23] Lee R. Dice, "Measures of the amount of ecologic association between species," *Ecology*, vol. 26, no. 3, pp. 297–302, 1945.